Electronic Supplementary Material (ESI) for Catalysis Science & Technology.

Different catalytic behavior of Pd and Pt metals in decalin dehydrogenation to naphthalene

Kyeounghak Kim[1], Jinho Oh[2], Tae Wan Kim[2], Ji Hoon Park[3], Jeong Woo Han[1,*], and Young-Woong Suh[2,4,*]

[1]Department of Chemical Engineering, University of Seoul, Seoul 02504, Republic of Korea
[2]Department of Chemical Engineering, Hanyang University, Seoul 04763, Republic of Korea
[3]Carbon Resources Institute, Korea Research Institute of Chemical Technology (KRICT), Daejeon 34114, Republic of Korea
[4]Research Institute of Industrial Science, Hanyang University, Seoul 04763, Republic of Korea

Supplementary Information

In order to verify the suitability of *k*-point sampling and van der waals (vdW) correction method used in our DFT calculations, we firstly examined the convergence of the adsorption energies of all adsorbates and the relative energy profile of dehydrogenation reaction from decalin to naphthalene with respect to *k*-point sampling (Fig. S1 and Table S1). Our results demonstrated that both the adsorption energies and the relative energy profile are well-converged at 2 × 2 × 1 *k*-point, which implies that the results would not be changed by increasing of *k*-point sampling. We also tested if the PBE-D3 method is appropriate to treat the vdW interaction of aromatic molecules with the surfaces in our system. Since the difference of catalytic activity can be partly determined by the difference in molecular adsorption energies on Pd and Pt surfaces, we compared the adsorption energies of all adsorbates on Pd and Pt surfaces using the lattice parameters optimized by PBE-D3, optPBE-vdW, and optB86b-vdW (Table S2). Our results showed that DFT-D3 describes well the vdW interaction, which is comparable to other methods such as optPBE-vdW and opt886b-vdW (Table S3).

E-mail. jwhan@uos.ac.kr (J.W. Han), ywsuh@hanyang.ac.kr (Y.-W. Suh)

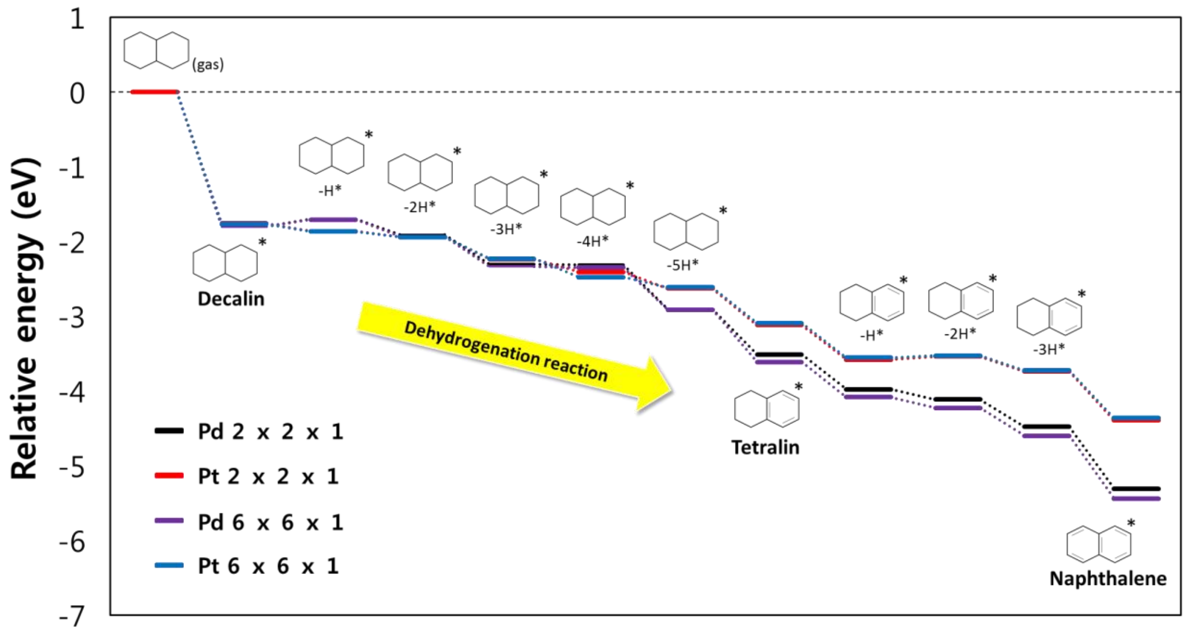

Figure S1: *k*-point convergence test of relative energy diagram for dehydrogenation reaction on Pd(111) and Pt(111).

k-point	2 x 2 x 1		4 x 4 x 1		6 x 6 x 1	
	Pd	Pt	Pd	Pt	Pd	Pt
Decalin	-1.98	-1.94	-1.92	-2.00	-1.97	-1.95
Tetralin	-2.26	-2.43	-2.30	-2.43	-2.33	-2.39
Naphthalene	-3.17	-3.19	-3.24	-3.18	-3.25	-3.13

Table S1: Adsorption energies (eV) of all adsorbates with respect to *k*-point sampling.

Lattice parameter (Å)	PBE-D3	optPBE-vdW	optB86b-vdW	Exp[b]
Pd	3.89 (3.89)[a]	3.96 (3.96)[a]	3.91 (3.91)[a]	3.88
Pt	3.93 (3.93)[a]	3.99 (3.99)[a]	3.95 (3.95)[a]	3.92

Table S2: Optimized lattice parameters for bulk Pd and Pt with regard to vdW functionals. The values superscripted by a and b are taken from “Curr. Appl. Phys. 15, 2015, 885-891.” and “Introduction to solid state physics, 8th Edition, Wiley, 2004.”, respectively.

	Decalin		Tetralin		Naphthalene	
	Pd	Pt	Pd	Pt	Pd	Pt
PBE-D3	-1.98	-1.94	-2.26	-2.43	-3.17	-3.19
optPBE-vdW	-1.56	-1.55	-1.87	-1.75	-2.34	-2.28 (-2.30)[a]
optB86b-vdW	-1.77	-1.73	-2.56	-2.51	-3.39	-3.40 (-3.39)[a]

Table S3: Adsorption energies (in eV) of decalin, tetralin, and naphthalene on Pd(111) and Pt(111) calculated by three different vdW corrections. The values superscripted by a are taken from "Phys. Chem. Chem. Phys. 17, 2015, 28921-28930."

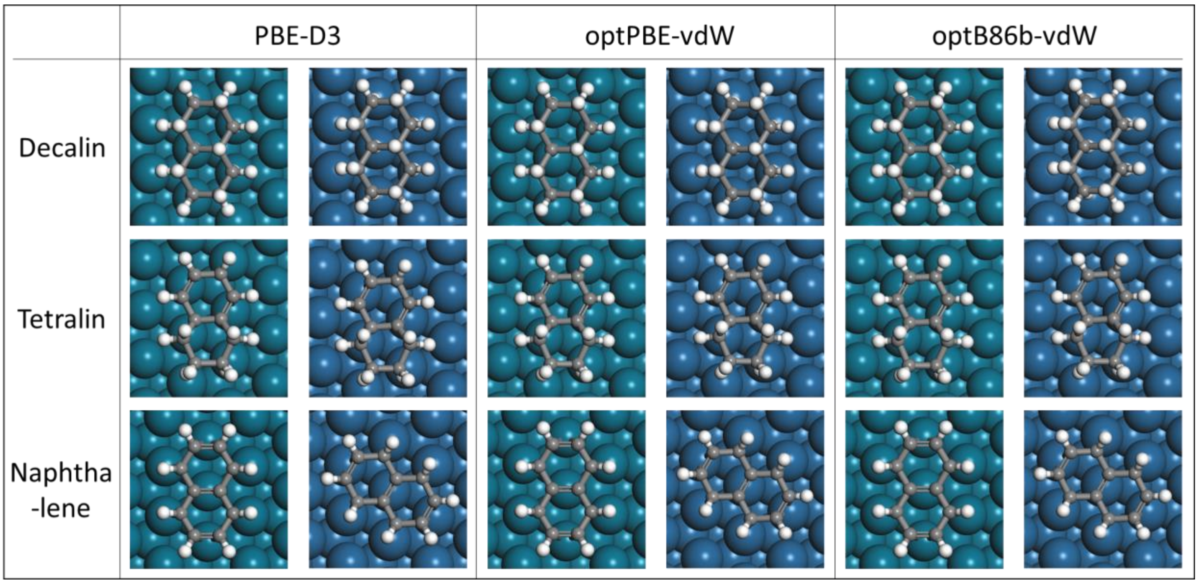

Figure S2: Optimized structures of decalin, tetralin, and naphthalene adsorbed on Pd(111) and Pt(111) calculated by three different vdW correction methods.

The adsorption geometries of decalin, tetralin, and naphthalene on Pd(111) and Pt(111) were systemically explored as shown in Fig. S3. The seven adsorption configurations of naphthalene on the metal surfaces were classified by the position of the centers of two aromatic rings and the azimuthal angles of the adsorbed molecule. Since decalin and tetralin also have two aromatic rings, we adopted the same procedure to examine their molecular adsorption structures. In our definition, the first and last characters of each name represent the position of ring centers such as top, bridge, fcc- or hcp-hollow sites. If the center of one aromatic ring is located above a top site, that of the other ring can be located at the two different bridge sites due to the asymmetric structure of the adsorbate's underlayer (fcc and hcp). In this case, we used one more character in the middle of their names with regard to the position of the center of aromatic ring located at the bridge site, which is denoted as TOP-FCC-Bridge and TOP-HCP-Bridge. We marked both sites by white crosses in Fig. S3. For example, in TOP-FCC-Bridge and TOP-HCP-Bridge configurations, fcc- and hcp-hollow sites are located at right near the centered two carbon atoms, respectively. When both aromatic rings are located at the bridge sites, two configurations are possible to the molecular adsorption; two centered carbon atoms are located at the bridge site between two surface atoms (Bridge1) or the top site of a surface atom (Bridge2). For the adsorption of dissociated atomic hydrogen, we examined top, bridge, hcp and fcc sites, respectively.

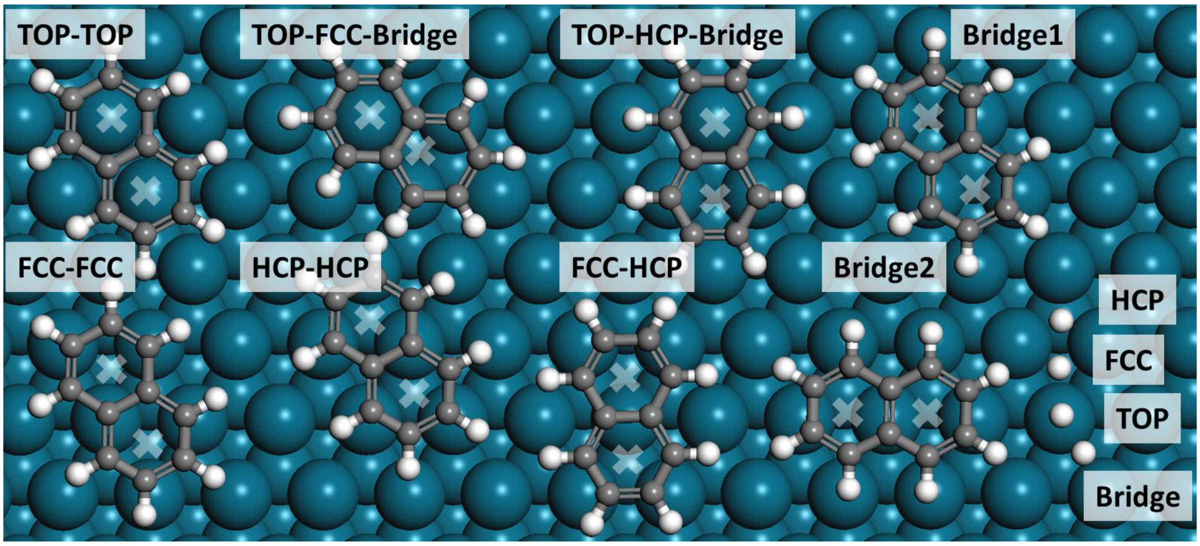

Figure S3: Considered adsorption sites for the adsorbates. We defined the adsorption configurations for each case of aromatic molecules depending on the position of two centers of aromatic rings. For better understanding, we marked white crosses at the representative points of the adsorption sites. For isolated hydrogen, we considered top, bridge, fcc-hollow, and hcp-hollow sites, respectively.

Contrary to tetralin or naphthalene, decalin has *cis*/*trans* isomers that two hydrogen atoms located at the center of molecule are headed for the same/opposite direction, respectively. In addition, we examined the two adsorption configurations of *cis*-decalin that two hydrogen atoms located at the center of molecule are headed in both down or up directions on metal surfaces, which are denoted as *cis-up*- and *cis-down*-decalin, respectively (Fig. S4).

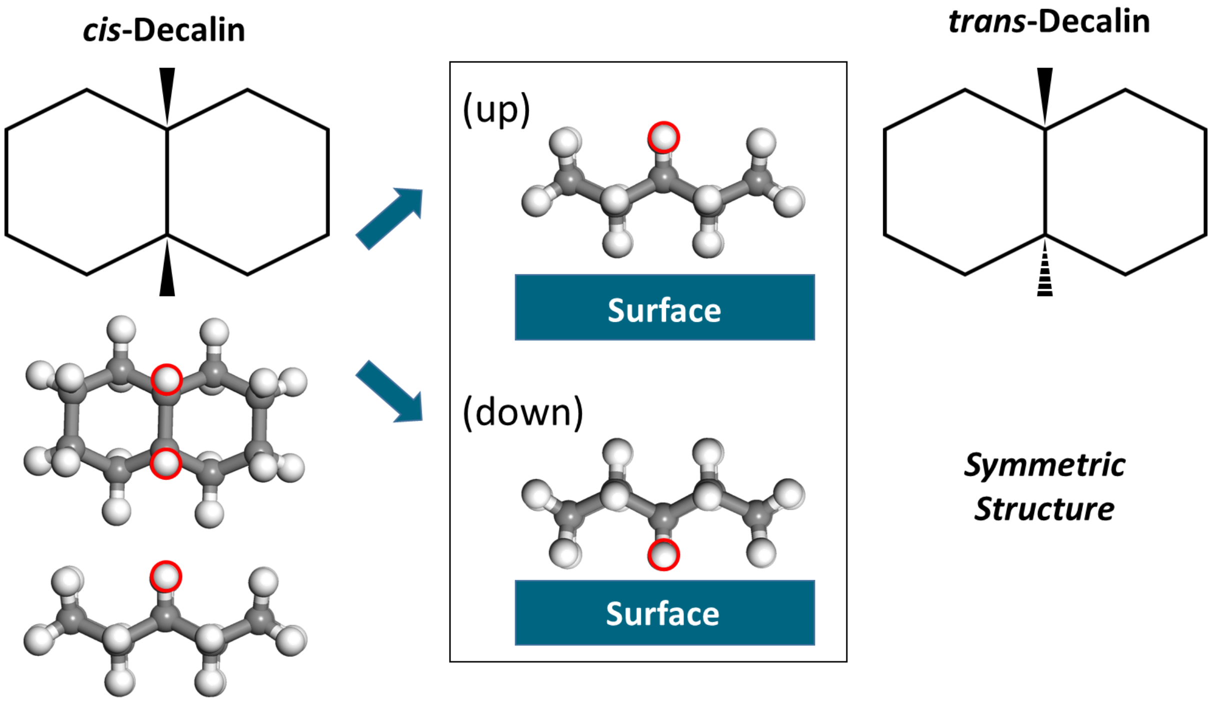

Figure S4: Two isomers and possible adsorption configurations of decalin. The black boxed figure in the middle is a schematic figure of molecule and surface configurations for *cis*-up- and *cis*-down-decalin adsorbed on metal surfaces. The red circle represents the direction of hydrogens far from or toward the metal surfaces.

To explore the characteristics of adsorption modes, we marked yellow double lines to the positions of π adsorption mode (Fig. S5). Since decalin is fully saturated, there is no π adsorption mode. However, the number of π adsorption modes increases as dehydrogenation proceeds. As can be seen in Fig. S3, tetralin has two π adsorption modes on both Pd(111) and Pt(111) while naphthalene exhibits three π adsorption modes on both surfaces, respectively.

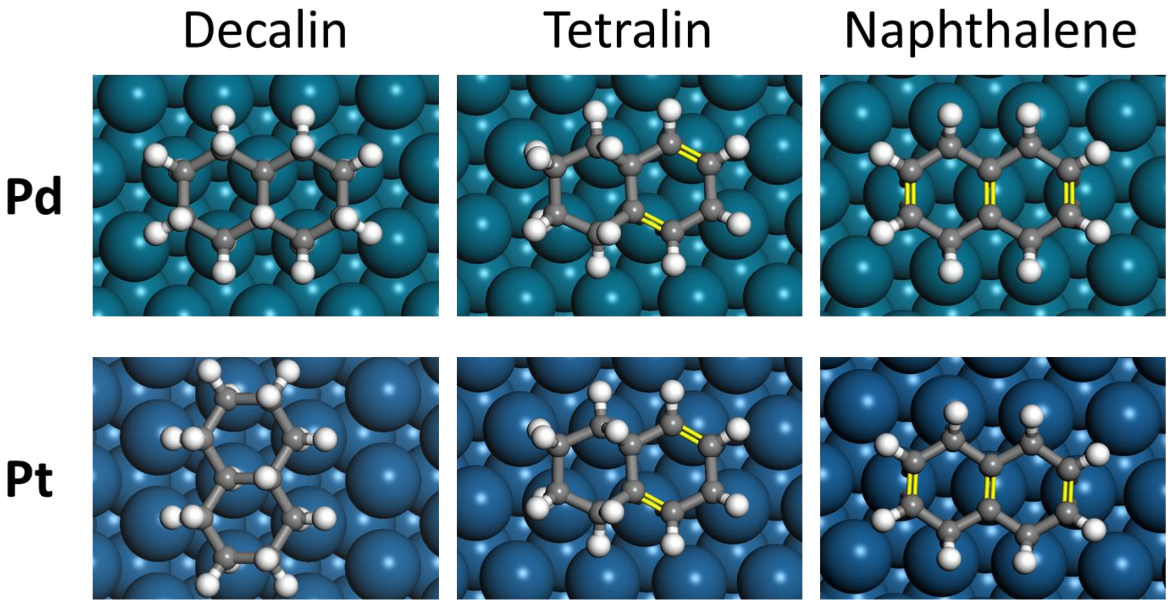

Figure S5: The optimized structures of decalin, tetralin, and naphthalene adsorbed on Pd(111) and Pt(111). The yellow stick represents a π adsorption mode.

We compared the molecular alignments between decalin and surface atoms upon the adsorption on both Pd(111) and Pt(111) (Fig. S6). Our results shows that the atomic alignment for the adsorption can be stabilized by the change of lattice constant of Pt(111) to that of Pd(111). This indicates that the atomic alignment significantly affects the molecular adsorption stability of decalin on both metal surfaces.

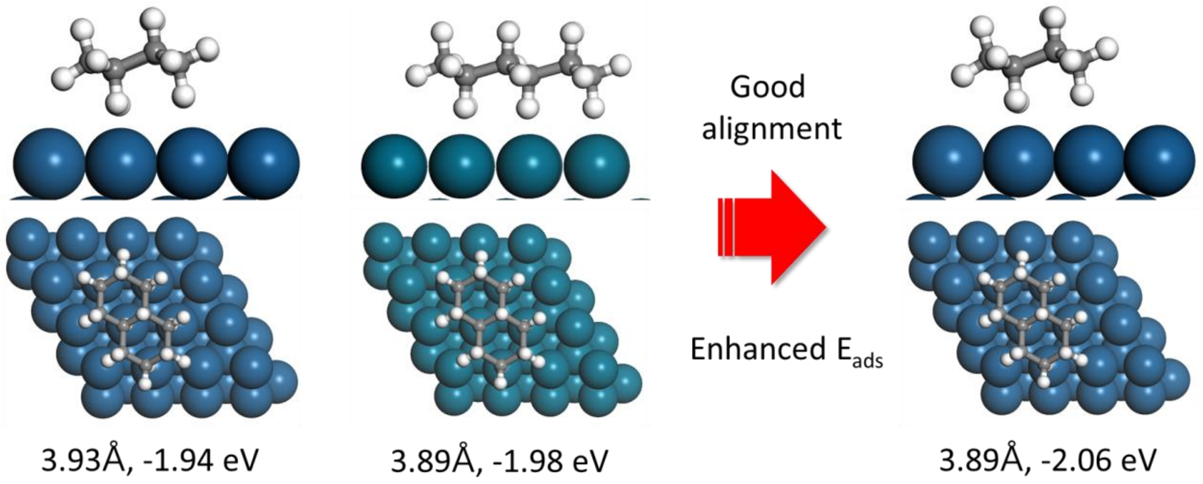

Figure S6: The side (up) and top view (down) of the optimized adsorption structures of decalin on Pt(111), Pt(111), and lattice modified Pt(111) from left to right, respectively. The dark blue and dark green represent Pt and Pd atoms, respectively.

To identify the sequence of dehydrogenation process, we examined the change of bond length of C–C (ΔC–C) in decalin, tetralin, and naphthalene for each dehydrogenation step. For better understanding of hydrogen decomposition site at each elementary step, we drew the figures for the sites in the right side of Table S3. We colored the numbers in red for the exception cases of dehydrogenated C–C bond where there is no noticeable decrease in C–C bond length. For these cases, we assumed that an additional bond is formed near the dehydrogenated carbon.

	Pt	Decalin	ΔC–C	H1	ΔC–C	H2	ΔC–C	H3	ΔC–C	H4	ΔC–C	H5	ΔC–C	Tetralin	ΔC–C
Decalin	$C_1 – C_2$	1.533	-0.018	1.530	-0.002	1.531	0.001	1.529	-0.002	1.543	0.014	1.520	-0.023	1.490	**-0.030**
	$C_2 – C_3$	1.529	0.003	1.529	0.000	1.537	0.008	1.513	-0.023	1.510	-0.003	1.511	0.001	1.483	-0.027
	$C_3 – C_4$	1.527	-0.023	1.524	-0.003	1.524	**0.000**	1.428	**-0.096**	1.428	0.000	1.427	-0.001	1.436	0.009
	$C_4 – C_5$	1.524	-0.011	1.524	0.000	1.522	-0.002	1.471	-0.051	1.473	0.002	1.474	0.001	1.471	-0.003
	$C_5 – C_6$	1.523	-0.010	1.525	**0.001**	1.524	-0.001	1.523	-0.001	1.518	-0.005	1.472	**-0.046**	1.470	-0.002
	$C_6 – C_1$	1.526	-0.028	1.522	-0.004	1.523	0.002	1.522	-0.002	1.532	**0.011**	1.429	-0.103	1.441	0.012
	Average	1.527	-0.015	1.526	-0.001	1.527	0.001	1.498	-0.029	1.501	0.003	1.472	-0.029	1.465	-0.007
	Pd	Decalin		H1		H2		H3		H4		H5		Tetralin	
	$C_1 – C_2$	1.534	-0.016	1.531	-0.003	1.529	-0.002	1.532	0.003	1.537	0.005	1.535	-0.002	1.465	**-0.070**
	$C_2 – C_3$	1.526	0.000	1.528	0.002	1.538	0.009	1.522	-0.016	1.520	-0.002	1.519	0.000	1.463	-0.057
	$C_3 – C_4$	1.525	-0.025	1.525	0.000	1.506	-0.019	1.440	**-0.066**	1.449	0.009	1.454	0.005	1.432	-0.022
	$C_4 – C_5$	1.527	-0.008	1.518	**-0.009**	1.397	**-0.122**	1.425	0.028	1.423	-0.001	1.434	0.010	1.450	0.016
	$C_5 – C_6$	1.526	-0.007	1.518	-0.008	1.504	-0.014	1.508	0.004	1.502	**-0.007**	1.450	-0.051	1.450	0.000
	$C_6 – C_1$	1.528	-0.026	1.525	-0.003	1.522	-0.002	1.525	0.003	1.527	0.002	1.468	**-0.059**	1.437	-0.032
	Average	1.528	-0.014	1.524	-0.003	1.499	-0.025	1.492	-0.007	1.493	0.001	1.477	-0.016	1.449	-0.027
	Pt	Tetralin		H1		H2		H3		Naphthalene					
Tetralin	$C_1 – C_2$	1.490	0.000	1.490	-0.001	1.475	-0.015	1.472	-0.003	1.470	-0.002				
	$C_2 – C_3$	1.513	0.030	1.493	**-0.021**	1.495	0.003	1.494	-0.002	1.470	-0.023				
	$C_3 – C_4$	1.520	0.084	1.523	0.003	1.519	-0.005	1.523	0.004	1.430	**-0.092**				
	$C_4 – C_5$	1.539	0.068	1.522	-0.017	1.529	0.007	1.523	-0.006	1.470	-0.052				
	$C_5 – C_6$	1.532	0.062	1.521	-0.011	1.506	-0.015	1.480	**-0.027**	1.475	-0.005				

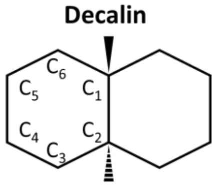

$C_6 - C_1$	1.526	0.085	1.530	0.004	1.434	**-0.096**	1.447	0.013	1.446	-0.001
Average	1.520	0.055	1.513	-0.007	1.493	-0.020	1.490	-0.003	1.460	-0.029
Pd	Tetralin		H1		H2		H3		Naphthalene	
$C_1 - C_2$	1.465	0.000	1.474	0.009	1.477	0.003	1.471	-0.007	1.461	-0.010
$C_2 - C_3$	1.512	0.050	1.466	**-0.046**	1.460	-0.007	1.458	-0.001	1.461	0.003
$C_3 - C_4$	1.524	0.092	1.517	-0.007	1.410	**-0.107**	1.428	0.017	1.448	0.020
$C_4 - C_5$	1.540	0.091	1.524	-0.016	1.506	-0.018	1.449	**-0.057**	1.426	-0.023
$C_5 - C_6$	1.533	0.083	1.524	-0.009	1.532	0.008	1.524	-0.008	1.446	**-0.078**
$C_6 - C_1$	1.523	0.086	1.525	0.002	1.524	-0.001	1.524	0.000	1.461	-0.063
Average	1.516	0.067	1.505	-0.011	1.485	-0.020	1.476	-0.009	1.451	-0.025

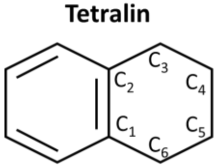

Table S3: The atomic bond distances of carbons (ΔC–C) in decalin, tetralin and naphthalene. Inner figures show the sequences of dehydrogenation process.

In addition, we investigated the relative reaction energy profiles of dehydrogenation processes on Pd(111) and Pt(111) for *cis-up-* (Fig. S7) and *cis-down*-decalin (Fig. S8). These cases also shows the same SDS steps in the first dehydrogenation process on Pd(111). Note that since there is no isomer for tetralin or naphthalene, the relative energy profiles for the second dehydrogenation process from tetralin to naphthalene are same for all cases. In the case of Pd, both *up-* and *down-* forms show the similar dehydrogenation sequence. Pd prefers to form the C=C double bond, which is consistent with the results of *trans*-decalin.

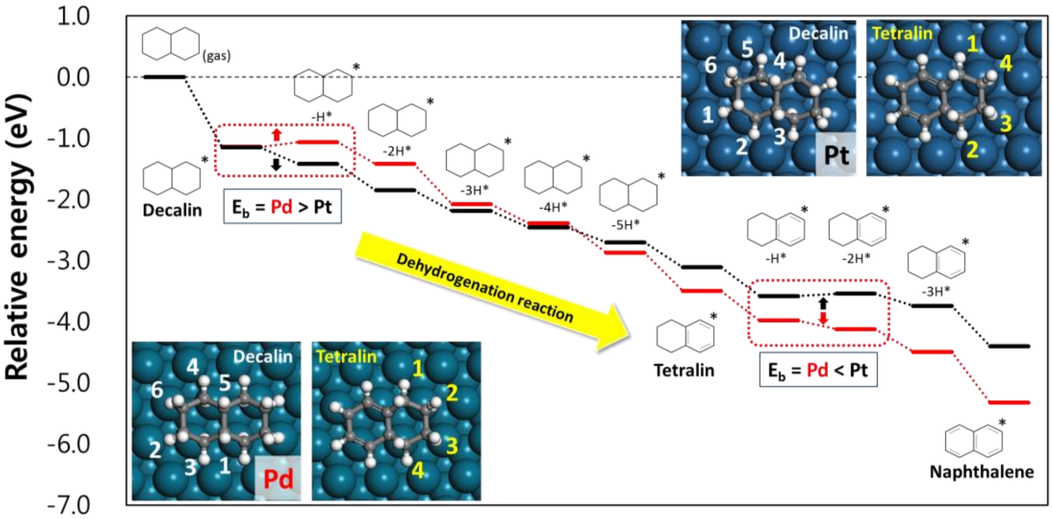

Figure S7: The relative energy diagram for dehydrogenation reaction on Pd(111) and Pt(111). The figure of up-right and down-left represent the optimized structure of *cis-up*-decalin and tetralin with the reaction sequence of dehydrogenation, respectively.

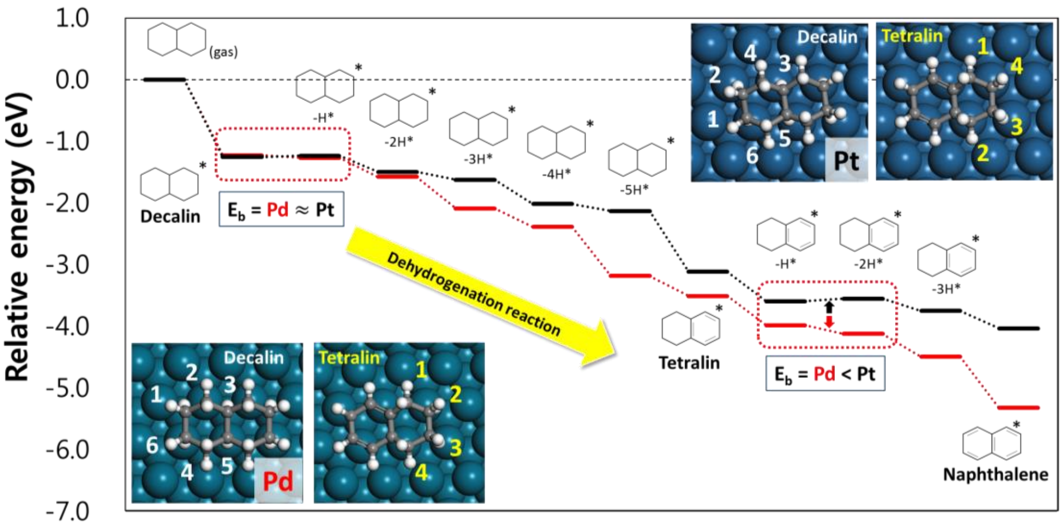

Figure S8: The relative energy diagram for dehydrogenation reaction on Pd(111) and Pt(111). The figure of up-right and down-left represent the optimized structure of *cis-down*-decalin and tetralin with the reaction sequence of dehydrogenation, respectively.

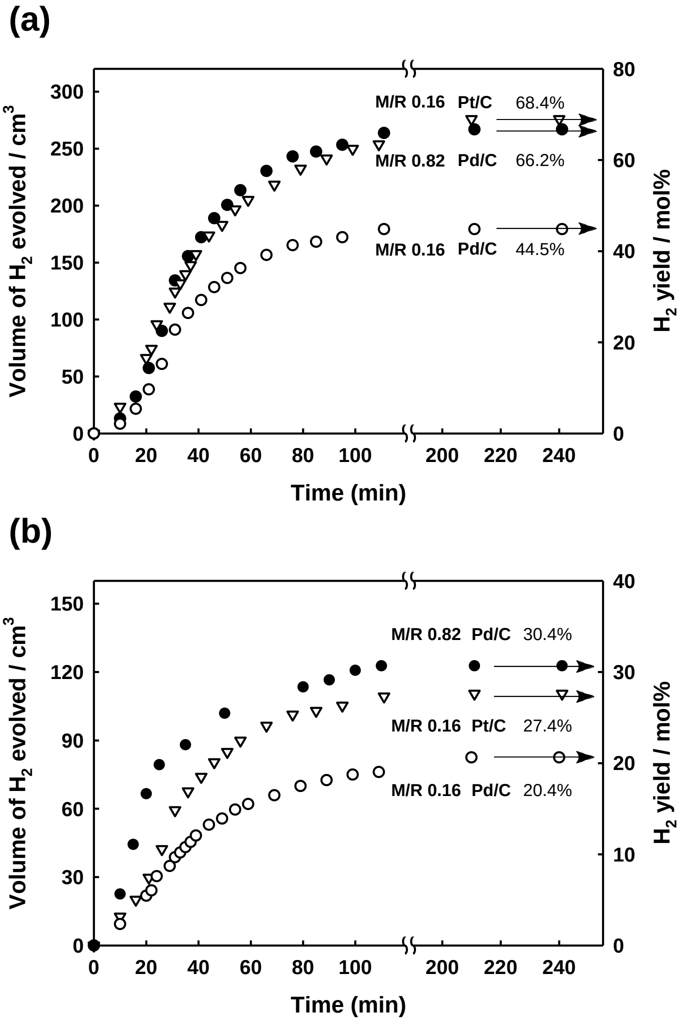

Figure S9: H_2 volume evolved as a function of the reaction time in the dehydrogenation of decalin over Pt/C and Pd/C at (a) 270 and (b) 250 °C. The calculation for H_2 yield was based on the theoretical volume of H_2 produced by complete conversion of decalin into naphthalene.

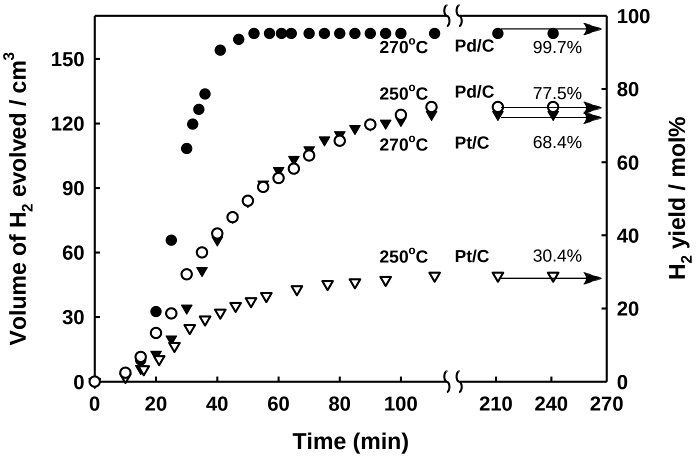

Figure S10: H_2 volume evolved as a function of the reaction time in the dehydrogenation of tetralin over Pt/C and Pd/C at 250 and 270 °C. The calculation for H_2 yield was based on the theoretical volume of H_2 produced by complete conversion of tetralin into naphthalene.